Propagating beam theory of optical fiber cross coupling

M. D. Feit and J. A. Fleck, Jr.

Lawrence Livermore National Laboratory, Livermore, California 94550

Received June 20, 1981

Evanescent field coupling between parallel optical waveguides is treated by the propagating beam method. This method utilizes Fourier analysis to generate the modal properties of optical waveguides from numerical solutions to the paraxial-wave equation. Previous applications have been for single waveguides. Detailed results are presented here for a variety of coupled waveguide pairs: identical slab waveguides, identical and nonidentical single-mode optical fibers, and identical few-mode optical fibers. Results include propagation constants and eigenfunctions for the normal modes of the coupled systems. The difference between the propagation constants of the corresponding normal modes determines the coupling length for the mode pair, whereas the eigenfunctions determine the extent of power transfer. The results obtained establish the applicability of the propagating beam method to the study of coupling in a general class of practical waveguides.

1. INTRODUCTION

The extension of guided-wave fields beyond confining core regions permits the exchange of energy between closely positioned optical waveguides. This electromagnetic coupling is both the origin of cross talk and the basis of directional waveguide couplers. In either case, the transverse coupling of optical waveguides has elicited wide interest for many years.

The exchange of electromagnetic energy between coupled transmission lines was analyzed first by Miller[1] and subsequently by Cook,[2] Fox,[3] and Louisell.[4] Field propagation in coupled parallel optical fibers was treated using coupled-mode theory by Jones,[5] Van Clooster and Phariseau,[6,7] Marcuse,[8] Snyder,[9] and Arnaud.[10] Cherin and Murphy,[11] however, studied the cross talk between highly multimoded optical fibers by using a quasi-ray technique. A more rigorous analysis of guided-wave modes in two parallel dielectric rods than is possible with coupled-mode theory was furnished by Wijngaard,[12] who computed the normal modes in terms of circular harmonics without explicit reference to the modes of an isolated rod. More recently, Yeh *et al.*[13] examined guided-wave propagation in two identical closely coupled fibers with the help of numerical solutions to the scalar paraxial-wave equation.

All the preceding methods have advantages and disadvantages. Coupled-mode theory in its most tractable form treats the coupling of only two modes—one mode for each of two parallel waveguides. This form of the theory gives a qualitatively accurate description of power transfer in many situations, but, since it does not properly take into account the deformation of the modes of the individual waveguides, it is applicable only when coupling between fibers is weak. This objection does not apply to the expansion method employed in Ref. 12, but for the latter method to be tractable, the expansions must be truncated at terms of reasonably low order with uncertain effects on accuracy. The ray-tracing techniques should provide useful information for multimode structures but would not be applicable to single- or few-mode waveguides.

The propagating beam approach of Ref. 13 gives detailed and accurate results when the method is applicable. One of its limitations is that it is applicable only when the axial distance for the transfer of power between the waveguides is of the order of the propagation distance that can be encompassed in an accurate computation. For fibers of practical interest, this computational distance is typically less than 10 cm. For assessing the cross talk of parallel waveguides, on the other hand, it may be necessary to deal with coupling distances of the order of kilometers. For multimode waveguides, computational results depend sensitively on input conditions and are difficult to interpret without precise knowledge of the modal composition of the fields and the beat distances for the individual modes.

For a description of guided-wave propagation in coupled waveguides that is accurate over all propagation distances of practical interest, it is thus essential to have accurate information on the *normal* modes, the modes of the combined waveguide system. This information includes both the propagation constants and the eigenfunctions. From the propagation constants one can determine the distances for the transfer of power corresponding to particular combinations of normal modes. From the eigenfunctions one can determine the completeness of this transfer.

The propagating beam method described in Refs. 14–17 was developed for generating precisely this kind of information from numerical solutions to the paraxial-wave equation. It is applicable under weak guidance conditions, or when $|\delta n/n| \ll 1$, which describes many systems of practical interest, and it combines accuracy, computational efficiency, and versatility. Although the applications that have been described thus far have been restricted to index profiles of circular symmetry, the method is equally applicable to general two-dimensional profiles. In fact, for problems involving two transverse dimensions, its advantages over more conventional methods become particularly apparent.

In this paper we outline the procedures for solving coupled waveguide problems with the propagating beam method, and we present numerical results for a variety of systems: coupled identical slab waveguides, coupled identical and nonidentical

0030-3941/81/111361-12$00.50

single-mode fibers, coupled identical three-mode fibers, and coupled identical six-mode fibers. The paper is organized as follows. Basic relations for the propagating beam method are reviewed in Section 2. Some general properties of coupled identical and nonidentical fibers are derived in Sections 3 and 4; conditions for maximal power localization and transfer are derived in Section 5. Initial conditions for the propagating fields are discussed in Section 6. Results for identical coupled slab waveguides are presented in Section 7, and the remainder of the paper is devoted to numerical examples involving coupled optical fibers.

2. BASIC RELATIONS FOR THE PROPAGATING BEAM METHOD APPLIED TO IDEAL LOSSLESS MEDIA

The propagating beam method of mode analysis is based on solutions of the paraxial-wave equation

$$2ik\frac{\partial \mathcal{E}'}{\partial z} = \nabla_1^2 \mathcal{E}' + k^2\left\{\left[\frac{n(x,y)}{n_0}\right]^2 - 1\right\}\mathcal{E}', \tag{1}$$

where $\mathcal{E}'$ is a complex field amplitude, $k = n_0\omega/c$, and n_0 is the refractive index of the cladding. One can also express $\mathcal{E}'(x, y, z)$ in terms of the set of orthonormal-mode eigenfunctions for the fiber as

$$\mathcal{E}'(x,y,z) = \sum_{n,j} A_{nj}u_{nj}(x,y)\exp(-i\beta'_n z), \tag{2}$$

where the index j is used to distinguish different modes within a degenerate set, the β'_n are propagation constants, and the coefficients A_{nj} are determined by the field at $z = 0$. The eigenfunctions $u_{nj}(x, y)$ are also eigenfunctions of the Helmholtz equation, and the corresponding propagation constants β_n can be determined from the expression

$$\beta_n = -k[1 - (1 + 2\beta'_n/k)^{1/2}], \tag{3}$$

which, however, is expressed relative to the value k. (To obtain the propagation constants in conventional usage, it is necessary to add k to the β_n values defined above.)

Knowledge of $\mathcal{E}'(x, y, z)$ makes it possible to compute the correlation function

$$\mathcal{P}_1(z) = \iint \mathcal{E}'^*(x,y,0)\mathcal{E}'(x,y,z)\mathrm{d}x\mathrm{d}y = \langle \mathcal{E}'^*(x,y,0)\mathcal{E}'(x,y,z)\rangle, \tag{4}$$

where the integration is carried out numerically over the waveguide cross section by using the trapezoidal rule. Substitution of Eq. (2) into Eq. (4) gives

$$\mathcal{P}_1(z) = \sum_{n,j} |A_{nj}|^2 \exp(-i\beta'_n z). \tag{5}$$

Multiplying Eq. (5) by the Hanning window function

$$w(z) = \begin{cases} 1 - \cos\dfrac{2\pi z}{Z} & 0 \le z \le Z \\ 0 & z > Z \end{cases} \tag{6}$$

and taking the Fourier transform with respect to z gives

$$\mathcal{P}_1(\beta) = \sum_n W'_n \mathcal{L}_1(\beta - \beta'_n), \tag{7}$$

where

$$W_n = \sum_j |A_{nj}|^2 \tag{8}$$

are the mode weights and

$$\mathcal{L}_1(\beta - \beta'_n) = \frac{\exp[i(\beta - \beta'_n)Z] - 1}{i(\beta - \beta'_n)Z} - 1/2\left\{\frac{\exp\{i[(\beta - \beta'_n)Z + 2\pi]\} - 1}{i[(\beta - \beta'_n)Z + 2\pi]} + \frac{\exp\{i[(\beta - \beta'_n)Z - 2\pi]\} - 1}{i[(\beta - \beta'_n)Z - 2\pi]}\right\}. \tag{9}$$

To determine the eigenvalues β'_n, it is necessary to solve Eq. (1) with an initial field distribution that avoids the excitation of modes with closely spaced eigenvalues.

The correlation function $\mathcal{P}_1(z)$ is generated simultaneously with the field $\mathcal{E}'(x, y, z)$. When the field has been propagated the desired axial distance Z, $\mathcal{P}_1(z)$ is multiplied by $w(z)$ and Fourier transformed to give $\mathcal{P}_1(\beta)$. Equation (7) can then be fitted to the data set for $\mathcal{P}_1(\beta)$, which determines the β'_n and W_n values. When high accuracy is required for the weight factors W_n, it may be necessary to use a mutivariate nonlinear least-squares fit, but for determining the propagation constants it can be assumed in nearly all cases that, in the neighborhood of an individual resonance, $\mathcal{P}_1(\beta)$ is accurately represented by

$$\mathcal{P}_1(\beta) = W_n \mathcal{L}_1(\beta - \beta'_n), \tag{10}$$

whence β'_n and W_n can be determined by a simple linear fitting procedure.[15] The single-resonance fit was used for all the numerical examples discussed in this paper.

If the exciting field has been chosen so that not more than one mode of a degenerate set is excited, the mode eigenfunctions can be evaluated by computing numerically the integral

$$u_{nj}(x,y) = \text{const} \times \int_0^Z \mathcal{E}'(x,y,z)w(z)\exp(i\beta'_n z)\mathrm{d}z = \text{const} \times \mathcal{E}'(x,y,\beta'_n), \tag{11}$$

which requires a prior determination of the β'_n values and an additional propagation calculation.

3. EVEN- AND ODD-PARITY MODES FOR A PAIR OF IDENTICAL OPTICAL FIBERS

The geometric configuration for two identical optical fibers is shown in Fig. 1. A reflection through the plane $x = 0$, which

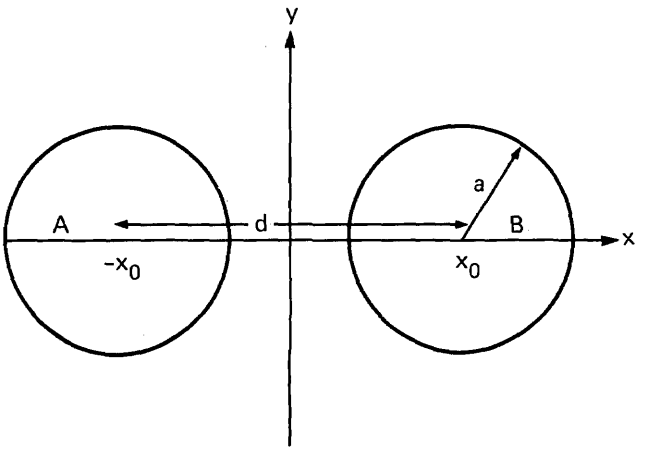

Fig. 1. Configuration for two identical circular symmetric fibers.

transforms (x, y) into (x', y'), where $x' = -x$ and $y' = y$, clearly leaves wave Eq. (1) invariant. As is well known, the mode eigenfunctions $u_{nj}(x, y)$ for this system must have the property

$$\mathcal{R}u_{nj}(x, y) = u_{nj}(-x, y) = \pm u_{nj}(x, y), \tag{12}$$

where the unitary operator $\mathcal{R}$ transforms $u_{nj}(x, y)$ in accordance with a reflection about the y axis. The two engenvalues ± 1 represent the parity (under reflection) of the modes, and we label the corresponding eigenfunctions $u^{+}_{nj}(x, y)$ and $u^{-}_{nj}(x, y)$.

If the two fibers are far apart, the corresponding even- and odd-parity modes are degenerate, with the common propagation constant

$$\beta'_{nj} = \beta'^{+}_{nj} = \beta'^{-}_{nj}, \tag{13}$$

where β'_{nj} is the propagation constant for a single isolated fiber. If the fibers are brought close together, the degeneracy is removed, and β'^{+}_{nj} and β'^{-}_{nj} take on distinct values. It should be noted that, even though the β'_{nj} are degenerate with respect to the index j, this degeneracy will also be removed as the fibers are brought together, and β'_{nj} will take on distinct values for the same n but differing j.

The linear combinations

$$u^{A}_{nj}(x, y) = u^{+}_{nj}(x, y) + u^{-}_{nj}(x, y), \tag{14a}$$

$$u^{B}_{nj}(x, y) = u^{+}_{nj}(x, y) - u^{-}_{nj}(x, y) \tag{14b}$$

leave most of the energy on one or the other fiber, which are arbitrarily labeled A and B. The evolution with respect to axial distance z of $u^{A}_{nj}(x, y)$ and $u^{B}_{nj}(x, y)$ is described by

$$u^{A}_{nj}(x, y, z) = \exp(i\beta^{+}_{nj}z)[u^{+}_{nj}(x, y) + \exp(-i\Delta\beta^{\pm}_{nj}z)u^{-}_{nj}(x, y)], \tag{15a}$$

$$u^{B}_{nj}(x, y, z) = \exp(i\beta^{+}_{nj}z)[u^{+}_{nj}(x, y) - \exp(-i\Delta\beta^{\pm}_{nj}z)u^{-}_{nj}(x, y)], \tag{15b}$$

where

$$\Delta\beta^{\pm}_{nj} = \beta'^{+}_{nj} - \beta'^{-}_{nj}. \tag{16}$$

Thus the intensity distribution for either linear combination varies periodically in such a way that almost all the power shifts back and forth from one fiber to the other with the period $L = 2\pi/\Delta\beta^{\pm}_{nj}$.

The propagation constants β'^{+}_{nj} and β'^{-}_{nj} can be expressed as

$$\beta^{\pm}_{nj} = \frac{\int u^{\pm *}_{nj} H u^{\pm}_{nj} \mathrm{d}x\,\mathrm{d}y}{\int u^{\pm *}_{nj} u^{\pm}_{nj} \mathrm{d}x\,\mathrm{d}y}, \tag{17}$$

where, in analogy with quantum mechanics, we have defined the Hamiltonian operator H as

$$H = \frac{1}{2k}\left(\frac{\partial^2}{\partial x^2} + \frac{\partial^2}{\partial y^2}\right) + \frac{k}{2}\left\{\left[\frac{n(x, y)}{n_0}\right]^2 - 1\right\}. \tag{18}$$

Equation (17) can be used to estimate the values of β'^{+}_{nj} and β'^{-}_{nj} if u^{+}_{nj} and u^{-}_{nj} are approximated by linear combinations of mode eigenfunctions for an isolated fiber, i.e.,

$$u^{\pm}_{nj}(x, y) = u^{A}_{nj}(x, y) \pm u^{B}_{nj}(x, y), \tag{19}$$

with

$$u^{A}_{nj}(x, y) \doteq u^{0}_{nj}(x, -x_A, y), \tag{20a}$$

$$u^{B}_{nj}(x, y) \doteq u^{0}_{nj}(x - x_B, y). \tag{20b}$$

Here the superscript zero designates an eigenfunction of an isolated fiber. Substitution of Eq. (19) into Eq. (17) yields

$$\beta'^{\pm}_{nj} = \beta'_{nj} + \frac{\langle u^{A*}V_B u^{A}\rangle + \langle u^{B*}V_A u^{B}\rangle \pm \langle u^{A*}V_A u^{B}\rangle \pm \langle u^{B*}V_B u^{A}\rangle}{2 \pm \langle u^{A*}u^{B}\rangle \pm \langle u^{B*}u^{A}\rangle}, \tag{21}$$

where for simplicity the subscripts of the eigenfunctions have been omitted and

$$V_{A,B} = \frac{k}{2}\left\{\left[\frac{n_{A,B}(x, y)}{n_0}\right]^2 - 1\right\}. \tag{22}$$

Here the subscripts A and B designate profiles centered at the appropriate fiber positions. With the neglect of $\langle u^{A*}V_B u^{A}\rangle$, $\langle u^{B*}V_A u^{B}\rangle$, $\langle u^{A*}u^{B}\rangle$, and $\langle u^{B*}u^{A}\rangle$, Eq. (21) reduces to the coupled-mode result[18]

$$\beta'^{\pm}_{nj} = \beta'_{nj} \pm c, \tag{23}$$

where the coupling constant c is defined by

$$c = \langle u^{A*}V_A u^{B}\rangle = \langle u^{B*}V_B u^{A}\rangle. \tag{24}$$

The necessity for neglecting certain integrals in order to derive the coupled-mode result is evidence that coupled-mode theory is valid only for modes that are weakly coupled. We shall not have occasion to apply Eq. (21) directly, but it will serve as a guide to which modes couple strongly.

4. PROPERTIES OF MODES FOR A PAIR OF NONIDENTICAL OPTICAL FIBERS

When the two fibers are not identical, the normal-mode eigenfunctions are no longer eigenfunctions of the unitary reflection operator $\mathcal{R}$ and thus cannot display simple even or odd parity. They may, however, display a kind of quasi-parity in which they resemble distorted versions of even- and odd-parity eigenfunctions if the fibers are close together but degenerate into functions localized on either one or the other fiber when the fibers are far apart.

To show this quasi-parity we express the normal-mode eigenfunctions in the form

$$u_{nj}(x, y) = u^{A}_{nj}(x, y) + \gamma u^{B}_{nj}(x, y), \tag{25}$$

where the constant γ is determined by invoking the stationarity condition

$$\delta\left[\frac{\langle (u^{A*}_{nj} + \gamma u^{B*}_{nj})H(u^{A}_{nj} + \gamma u^{B}_{nj})\rangle}{\langle (u^{A*}_{nj} + \gamma u^{B*}_{nj})(u^{A}_{nj} + \gamma u^{B}_{nj})\rangle}\right] = 0. \tag{26}$$

By applying Eq. (26) in conjunction with Eqs. (20a) and (20b) and neglecting $\langle u^{A*}V_B u^{A}\rangle$, $\langle u^{B*}V_A u^{B}\rangle$, $\langle u^{A*}u^{B}\rangle$, and $\langle u^{B*}u^{A}\rangle$, one obtains the following two values for γ:

$$\gamma^{\pm} = -\frac{\beta'^{A}_{nj} - \beta'^{B}_{nj}}{2c} \pm \left[\left(\frac{\beta'^{A}_{nj} - \beta'^{B}_{nj}}{2c}\right)^2 + 1\right]^{1/2}, \tag{27}$$

where β'^{A}_{nj} and β'^{B}_{nj} are the propagation constants for the isolated fibers, and

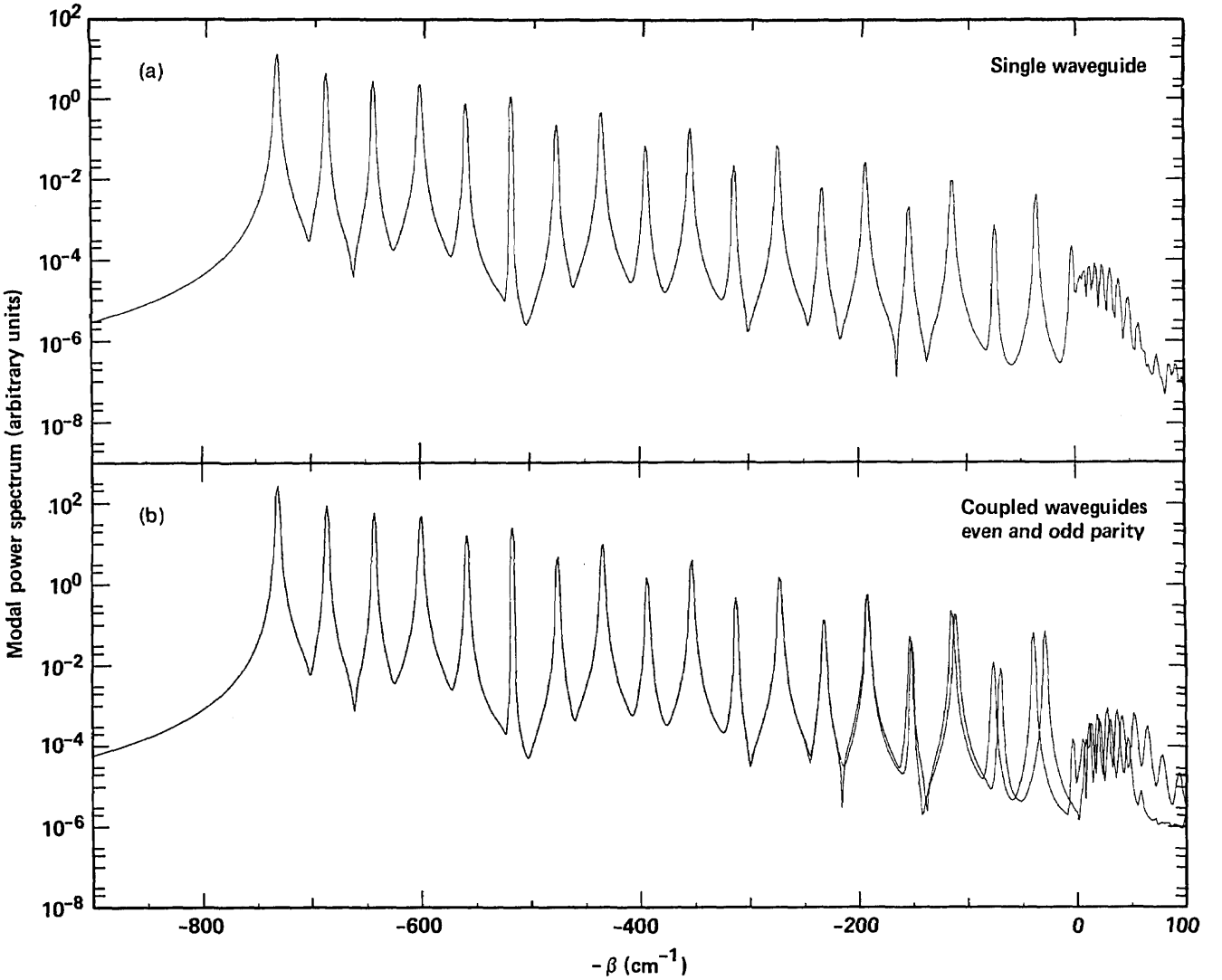

Fig. 2. (a) Mode spectra for single waveguide and (b) for two identical waveguides whose cores are just in contact. Spectra for even- and odd-parity modes have been superposed.

$$2c = \langle u^{A*} V_A u^B \rangle + \langle u^{B*} V_B u^A \rangle. \tag{28}$$

[Phases can always be selected so that the phase of Eq. (28) vanishes.] In the limit as $(\beta'^A_{nj} - \beta'^B_{nj})/2c$ becomes small, or when the fibers approach one another, γ approaches ± 1, and Eq. (25) displays even or odd parity. In the limit as $(\beta'^A_{nj} - \beta'^B_{nj})/2c$ becomes large, or as the distance between fibers increases, γ^+ and γ^- approach $c/(\beta'^A_{nj} - \beta'^B_{nj})$ and $-(\beta'^A_{nj} - \beta'^B_{nj})/c$, respectively. In other words, as the field evolves with axial distance, the power continues to be associated primarily with one fiber, with little power transferring to the other fiber. This contrasts with the behavior of identical fibers, which periodically exchange their power almost completely, even for large fiber separations.

If Eq. (25) is substituted into Eq. (17) and the approximations used in the derivation of Eq. (27) are applied, the familiar coupled-mode result[17]

$$\beta'^{\pm}_{nj} = 1/2(\beta'^A_{nj} + \beta'^B_{nj}) \pm [1/4(\beta'^A_{nj} - \beta'^B_{nj})^2 + c^2]^{1/2} \tag{29}$$

is obtained. As c becomes small in comparison with $\beta'^A_{nj} - \beta'^B_{nj}$, β'^+_{nj} and β'^-_{nj} assume the values β'^A_{nj} and β'^B_{nj} that are appropriate to isolated fibers, which is consistent with the behavior of the corresponding normal-mode eigenfunctions [Eq. (25)].

5. CONDITIONS FOR MAXIMAL POWER LOCALIZATION AND TRANSFER

We wish to determine the linear combination of normal modes

$$u(x, y) = u^+(x, y) + Gu^-(x, y) \tag{30}$$

that (1) maximizes the power in one or the other fiber and (2) maximizes the fractional power transfer from one fiber to the other. Here $u^+(x, y)$ and $u^-(x, y)$ are normalized eigenfunctions for associated normal modes of coupled fibers, which may or may not be identical. For simplicity we have ignored subscripts.

To maximize the power in fiber B, we choose G to maximize the integral

$$\frac{1}{1+G^2}\int_0^\infty \int_{-\infty}^\infty u^2(x, y)\,dx\,dy = \frac{\langle (u^+ + Gu^-)^2 \rangle^+}{1+G^2}$$
$$= \frac{\langle u^{+2} \rangle^+ + 2G\langle u^+ u^- \rangle^+ + G^2 \langle u^{-2} \rangle^+}{1+G^2}, \tag{31}$$

where the superscript + on the angle brackets denotes integration over the right half-plane and $u^+(x, y)$ and $u^-(x, y)$ have been chosen to be real. The appropriate value of G is

$$G_B = -1/2\,\frac{\langle u^{+2}\rangle^+ - \langle u^{-2}\rangle^+}{\langle u^+u^-\rangle^+} + \left[\left(\frac{\langle u^{+2}\rangle^+ - \langle u^{-2}\rangle^+}{2\langle u^+u^-\rangle^+}\right)^2 + 1\right]^{1/2}. \quad (32)$$

For identical fibers that are not too close, G will be accurately approximated by 1. For nonidentical fibers that are far apart, on the other hand, $|G_B| \ll 1$, and

$$G_B = \frac{\langle u^+u^-\rangle^+}{\langle u^{+2}\rangle - \langle u^{-2}\rangle^+}. \quad (33)$$

The fraction of power associated with fiber B after the field has propagated a distance z can be written as

$$P_B = \frac{\langle|u^+ + G\exp(-i\Delta\beta^{\pm}z)u^-|^2\rangle^+}{1+G^2} = \frac{\langle u^{+2}\rangle^+ + G^2\langle u^{-2}\rangle^+}{1+G^2} + \frac{2G\cos(\Delta\beta^{\pm}z)\langle u^+u^-\rangle^+}{1+G^2}. \quad (34)$$

The variation of P_B over the distance $\pi/\Delta\beta^{\pm}$ and, consequently, the fractional power transfer from fiber B to fiber A is

$$\Delta P_B = 4\,\frac{G}{1+G^2}\,\langle u^+u^-\rangle^+, \quad (35)$$

which is maximized when $G = 1$. In that case

$$\Delta P_{B\,\max} = 2\langle u^+u^-\rangle^+. \quad (36)$$

The field

$$u(x,y) = u^+(x,y) + u^-(x,y) \quad (37)$$

thus maximizes the power transfer for both identical and nonidentical fibers. However, the field [Eq. (37)] maximizes both power flow and power concentration simultaneously only if the fibers are identical.

Table 1. Splitting Values ($\Delta\beta^{\pm} = \beta_n^{\prime+} - \beta_n^{\prime-}$) between Propagation Constants for Positive- and Negative-Parity Normal Modes for Two Equivalent Touching Slab Waveguides Computed for Two Propagation Distances

Mode (n)	$\Delta\beta^{\pm}$ (cm^{-1})[a]	$\Delta\beta^{\pm}$ (cm^{-1})[b]
0	—	—
1	—	—
2	3.27418×10^{-11}	5.09317×10^{-11}
3	1.32059×10^{-9}	1.1205×10^{-9}
4	2.1300×10^{-8}	2.14131×10^{-8}
5	2.97900×10^{-7}	2.97943×10^{-7}
6	3.27527×10^{-6}	3.27606×10^{-6}
7	2.93923×10^{-5}	2.93904×10^{-5}
8	2.19158×10^{-4}	2.18996×10^{-4}
9	1.37667×10^{-3}	1.37675×10^{-3}
10	7.36793×10^{-3}	7.36869×10^{-3}
11	3.3827×10^{-2}	3.38251×10^{-2}
12	1.33500×10^{-1}	1.33673×10^{-1}
13	4.55580×10^{-1}	4.55606×10^{-1}
14	1.33469×10^{0}	1.33484×10^{0}
15	3.31488×10^{0}	3.31487×10^{0}
16	6.73585×10^{0}	6.73585×10^{0}
17	1.06880×10^{1}	1.06880×10^{1}

[a] Computation made with $Z = 4.096$ cm.
[b] Computation made with $Z = 8.192$ cm.

6. CHOOSING INITIAL CONDITIONS FOR EXCITING SPECIFIC MODE SETS

Since corresponding even- and odd-parity modes for pairs of identical waveguides are almost degenerate, it may be necessary to generate the even- and odd-parity modes independently to avoid the overlap of resonances in the spectrum $\mathcal{P}_1(\beta)$. For identical multimode slab waveguides, the complete spectra for all bound even- and odd-parity modes can be generated in a pair of computer runs, with the initial conditions for Eq. (1) in the form

$$\mathcal{E}'(x,0) = \mathcal{E}_0'(x - x_0) \pm \mathcal{E}_0'(x + x_0), \quad (38)$$

where $\mathcal{E}_0'(x)$ is a general suitably well-behaved function.

For two identical optical fibers, the counterpart to Eq. (24) is

$$\mathcal{E}'(x,y,0) = \mathcal{E}_0'(x - x_0, y) \pm \mathcal{E}_0'(x + x_0, y). \quad (39)$$

If the fibers are single mode, there is no problem in applying condition (39). If the fibers are multimode, the possibility exists of fortuitously exciting nearly degenerate normal modes. Thus selecting $\mathcal{E}_0'(x,y)$ is not as simple as selecting $\mathcal{E}_0'(x)$. One approach is to form the initial field from one or more symmetric and antisymmetric combinations of appropriately centered single-fiber eigenfunctions, i.e.,

$$\mathcal{E}'(x,y,0) = u_{nj}^0(x - x_0, y) \pm u_{nj}^0(x + x_0, y), \qquad j = 1, 2, \ldots, J, \quad (40)$$

where J is the degree of degeneracy.

A problem immediately arises because linear combinations of the degenerate eigenfunctions within a set are in principle equally appropriate for use in Eq. (40). Not all linear combinations or representations, however, are equally useful. For an appropriate representation, imposition of the initial conditions of Eq. (40) will excite an assortment of normal modes but with one mode predominating in amplitude. The task of resolving the normal-mode resonances and identifying the normal modes will clearly be simpler than for the case in which a number of almost degenerate normal modes are excited with comparable amplitudes.

If we consider, for example, two identical optical fibers with parabolic-index profiles,

$$n^2 = \begin{cases} n_1^2\left[1 - 2\Delta\left(\dfrac{r}{a}\right)^2\right] & r \le a \\ n_0^2 = (1 - 2\Delta)n_1^2 & r \ge a \end{cases}, \quad (41)$$

where r is measured from the appropriate local fiber center, the degenerate unperturbed eigenfunctions can be expressed in representations appropriate to either Cartesian or polar coordinates. The former functions are

$$u_{mn}(x,y) = (\pi 2^{n+m}m!n!)^{-1/2} \times \exp[-(x^2 + y^2)/2\sigma_a^2]H_m(x/\sigma_a)H_n(y/\sigma_a), \quad (42)$$

where $H_m(x)$ and $H_n(y)$ are Hermite polynomials and

$$\sigma_a = \left[\frac{a}{k(2\Delta)^{1/2}n_1/n_0}\right]^{1/2}. \quad (43)$$

The latter functions are

$$u_\mu^\nu(r,\theta) = e^{i\nu\theta}\exp(-r^2/2\sigma_a^2)(r/\sigma_a)^\nu L_\mu^\nu(r^2/\sigma_a^2), \quad (44)$$

Table 2. Propagation Constants for Even-Parity Normal Modes of Two Coupled Slab Waveguides Computed for Two Propagation Distances

Mode (n)	$\beta_n'^{+}$ (cm^{-1})[a]	$\beta_n'^{+}$ (cm^{-1})[b]	Change (cm^{-1})
0	7.30617×10^2	7.30617×10^2	-1.74×10^{-6}
1	6.85889×10^2	6.85889×10^2	-2.43×10^{-6}
2	6.42891×10^2	6.42892×10^2	-3.06×10^{-6}
3	6.00433×10^2	6.00433×10^2	6.02×10^{-6}
4	5.58535×10^2	5.58535×10^2	4.12×10^{-6}
5	5.16953×10^2	5.16952×10^2	-1.10×10^{-6}
6	4.75700×10^2	4.75699×10^2	-1.17×10^{-5}
7	4.34670×10^2	4.34671×10^2	3.22×10^{-6}
8	3.93873×10^2	3.93873×10^2	3.45×10^{-5}
9	3.53250×10^2	3.53250×10^2	4.63×10^{-6}
10	3.12807×10^2	3.12807×10^2	2.66×10^{-5}
11	2.72516×10^2	2.72516×10^2	6.64×10^{-6}
12	2.32410×10^2	2.32410×10^2	3.38×10^{-4}
13	1.92552×10^2	1.92552×10^2	3.18×10^{-5}
14	1.53157×10^2	1.53157×10^2	1.09×10^{-4}
15	1.14577×10^1	1.14578×10^1	2.11×10^{-5}
16	7.70496×10^1	7.70497×10^1	3.80×10^{-5}
17	4.00510×10^0	4.00510×10^0	2.52×10^{-6}

[a] $Z = 4.096$ cm.
[b] $Z = 8.192$ cm.

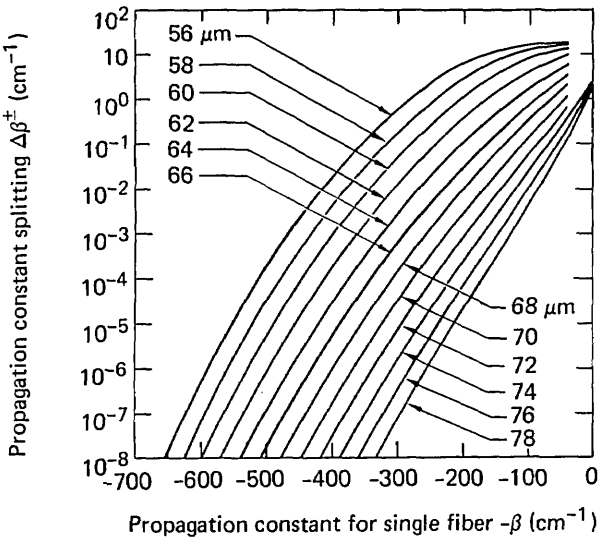

Fig. 3. Plot of difference $\Delta\beta^{\pm}$ of even- and odd-parity normal-mode propagation constants for differing separations. The beat distance or distance for energy transfer between fibers is $L = \pi(\Delta\beta^{\pm})^{-1}$.

where $L_\mu^\nu(x)$ is a generalized Laguerre polynomial. The members of either set can, in any case, be expressed as linear combinations of members of the other set. The set in Eq. (42), however, is clearly more appropriate for use in Eq. (40) than the set in Eq. (44) since only the former set exhibits the reflection symmetry with respect to the x and y axes required by the Hamiltonian H.

If one is treating coupled identical highly multimoded fibers, some of the unperturbed higher-order modes of the isolated fibers will necessarily be highly degenerate, making the task of identifying and classifying the normal modes difficult and complex.

The selection of initial conditions for coupled nonidentical fibers is even less amenable to generalization. Since the normal modes for this case are neither of purely even nor odd parity, it will be impossible to avoid exciting simultaneously the modes corresponding to $u^+(x, y)$ and $u^-(x, y)$. If the fibers are sufficiently close, the separation of the propagation constants is large, and there is no problem in resolving the mode resonances. If the fibers are far apart, the input field can be taken as a mode eigenfunction for one or the other fiber, appropriately centered.

7. COUPLING OF IDENTICAL SLAB WAVEGUIDES

We consider the coupling of two identical slab waveguides with refractive-index profiles

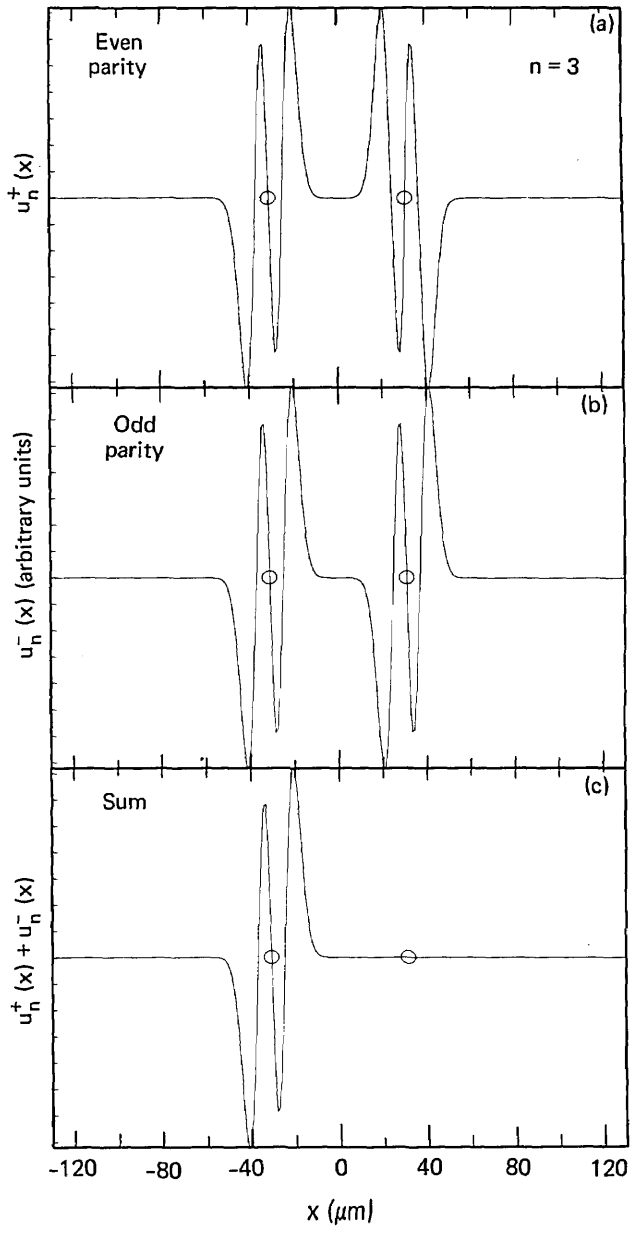

Fig. 4. Normal-mode eigenfunctions for two similar coupled planar waveguides and $n = 3$. (a) Even parity, (b) odd parity, (c) sum of even- and odd-parity eigenfunctions.

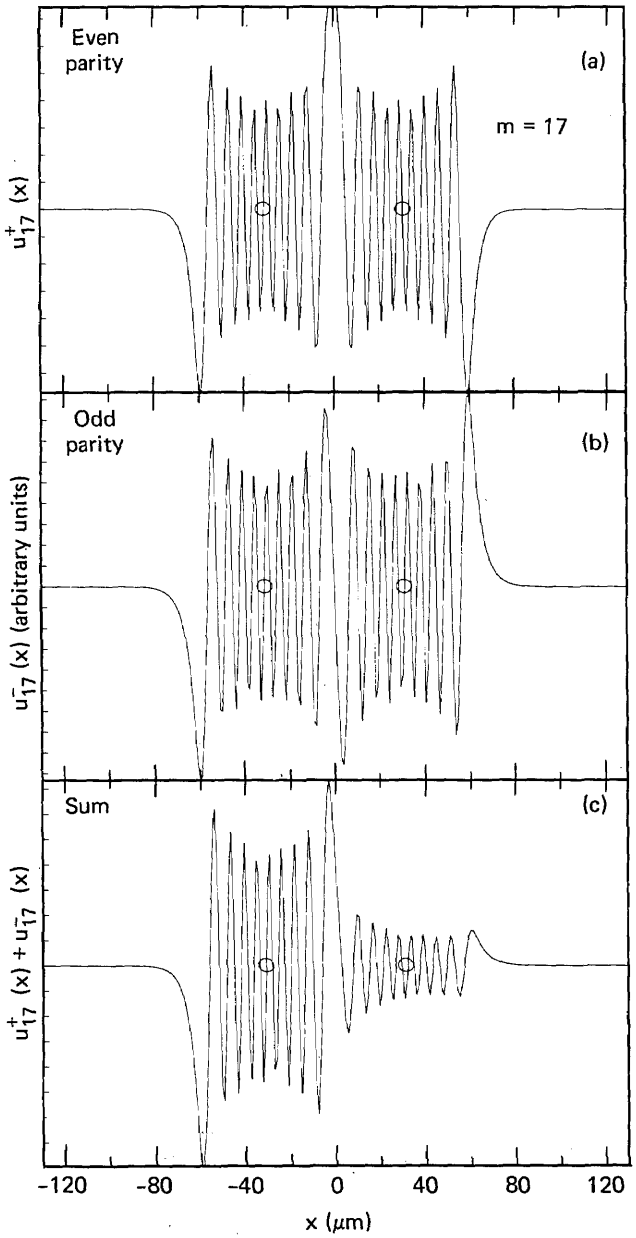

Fig. 5. Normal-mode eigenfunctions ($n = 17$) for coupled identical planar waveguides. (a) Even-parity mode, (b) odd-parity mode, (c) sum of even- and odd-parity eigenfunctions.

Table 3. Propagation Constants (β'^{+}, β'^{-}) and Splitting ($\Delta\beta^{\pm} = \beta'^{+} - \beta'^{-}$) Computed for Two Coupled Identical Single-Mode Fibers as a Function of Separation of Centers d

d (μm)	β'^{+} (cm^{-1})	β'^{-} (cm^{-1})	$\Delta\beta^{\pm}$ (cm^{-1})
∞	27.50985	27.50985	0
14	29.92722	24.65465	5.27257
10	34.52299	18.96165	15.56134

$$n^2 = \begin{cases} n_1^2\left[1 - 2\Delta\left(\dfrac{x}{a}\right)^{\alpha}\right] & x \le a \\ n_0^2 = (1 - 2\Delta)n_1^2 & x \ge a \end{cases}, \qquad (45)$$

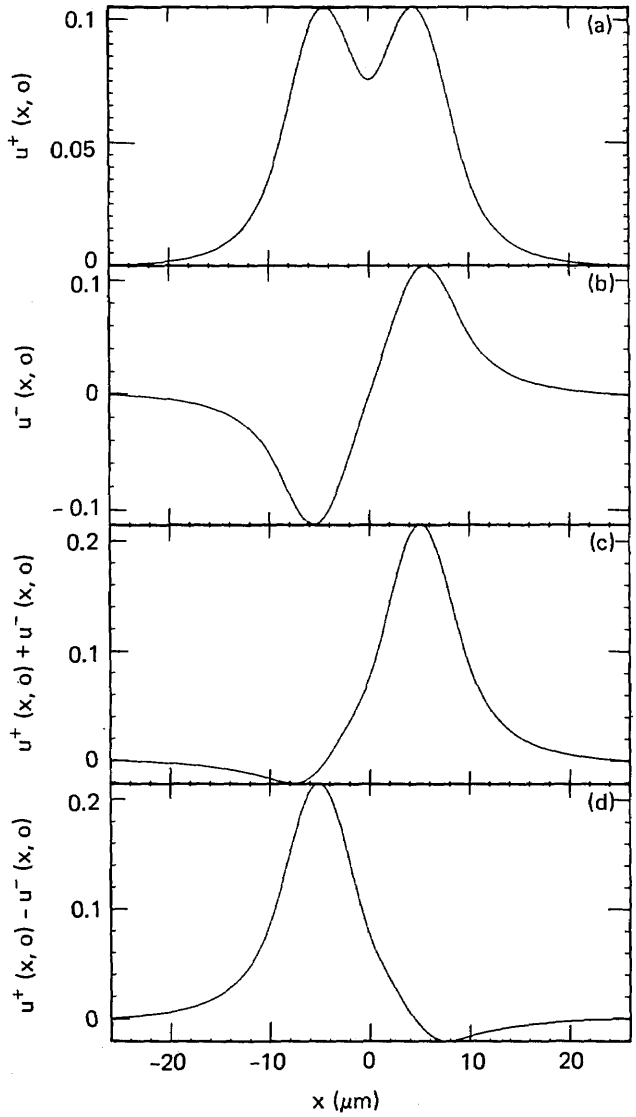

Fig. 6. Normal-mode eigenfunctions for two coupled identical single-mode fibers plotted along a line connecting their centers. Fiber cores are just in contact. (a) Even-parity mode, (b) odd-parity mode, (c) sum, (d) difference. Fractional distribution of power on two fibers corresponding to (c) and (d) is 0.03748 and 0.96252.

Table 4. Propagation Constants for Coupled Nonidentical Single-Mode Fibers as a Function of Separation d

d (μm)	β'^{+} (cm^{-1})	β'^{-} (cm^{-1})	$\Delta\beta^{\pm}$ (cm^{-1})
∞	27.50985	19.09500	8.41485
21	27.53110	18.86732	8.66378
11	30.56741	14.53923	16.02818

where $\alpha = 1.85$, $a = 31.25\ \mu$m, $\Delta = 7.873 \times 10^{-3}$, and $n_0 = 1.5$. The waveguide centers are separated by a distance d that was varied from 56 to 78 μm. A vacuum wavelength $\lambda = 1\mu$m was assumed, and propagation of the field was computed for axial distances $Z = 4.096$ cm and $Z = 8.192$ cm, covered in 10-μm increments. The function $\mathcal{E}_0'(x)$ used in Eq. (24) was

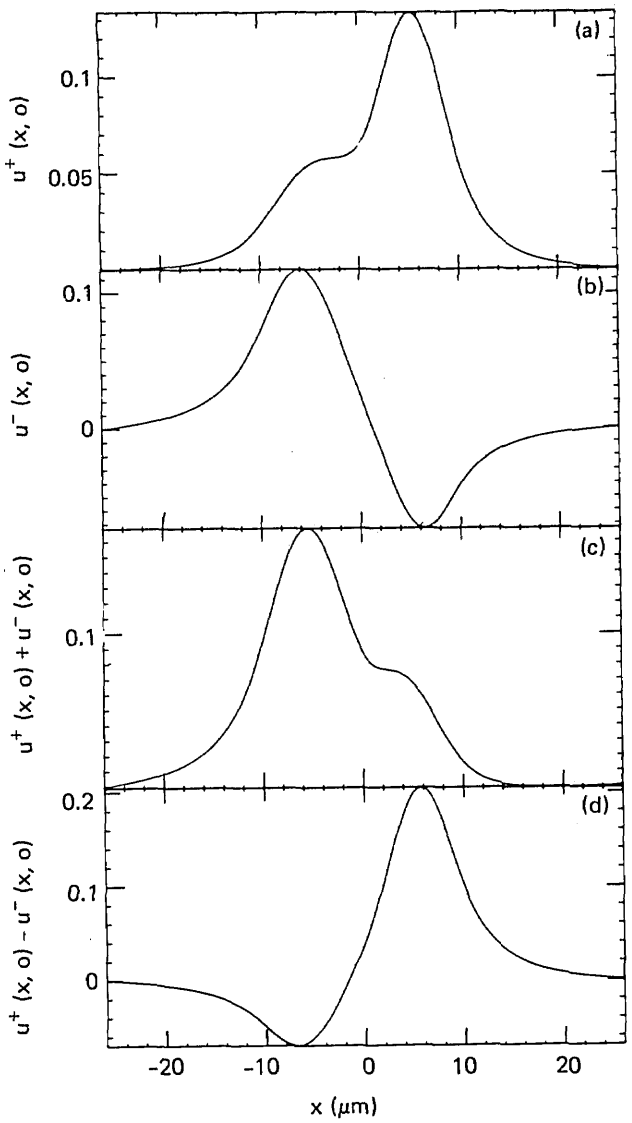

Fig. 7. Normal-mode eigenfunctions for two nonidentical single-mode fibers. Fiber cores are just in contact. (a) $u^+(x, 0)$ displays quasi-even parity; (b) $u^-(x, 0)$ displays quasi-odd parity; (c) sum; (d) difference.

$$\mathcal{E}_0'(x) = (1 + x)\exp(-x^2/2\sigma^2), \tag{46}$$

with $\sigma = 10.24$ μm. If Eq. (46) is the input to a single waveguide, it will excite both even- and odd-parity (single waveguide) modes. Thus Eq. (46) in conjunction with Eq. (24) will allow the excitation of all normal modes in a pair of propagation runs.

The spectrum $|\mathcal{P}_1(\beta)|$ for a single isolated waveguide is plotted versus $-\beta$ in Fig. 2(a). The spectra for the even- and odd-parity normal modes for two identical coupled waveguides are superposed in Fig. 2(b). The assumed separation is $d = 62$ μm, corresponding to the waveguide cores in contact with each other. A total of 18 bound modes for the single waveguide is evident in Fig. 2(a). The corresponding even- and odd-parity normal modes can be identified in Fig. 2(b), in which the odd-parity resonances are displaced slightly toward $\beta = 0$. The splitting of the normal-mode eigenvalues, $\Delta\beta^+ = \beta_n'^+ - \beta_n'^-$, is visible for the highest 4 or 5 orders of bound modes but is generally imperceptible for lower-order normal modes.

The $\Delta\beta^\pm$ values for individual normal modes, computed for two propagation distances, are presented in detail in Table 1. Since the accuracy of propagation constants determined from the locations of resonances improves with propagation distance, computations were made with two values of Z to test the accuracy of the computed splittings. The splitting values, except those for the three lowest-order modes, are found to be surprisingly insensitive to propagation distance, which leads to confidence in their values. The sensitivity to propagation distance of the propagation constants of the even-parity normal modes is exhibited in Table 2. The implied uncertainty in the propagation constants ranges from 10^{-4} cm^{-1} to 10^{-6} cm^{-1}. The fact that the splitting values may exhibit less sensitivity to distance than the propagation constants from which they are derived results from the cancellation of systematic errors.

The splitting $\Delta\beta^\pm$ is plotted as a function of propagation constant for a single isolated waveguide in Fig. 3 for a range of d values. From Fig. 3, it can be concluded that the power coupling distance $L = \pi(\Delta\beta^\pm)^{-1}$ can be a strong function of propagation constant or mode number. From these results

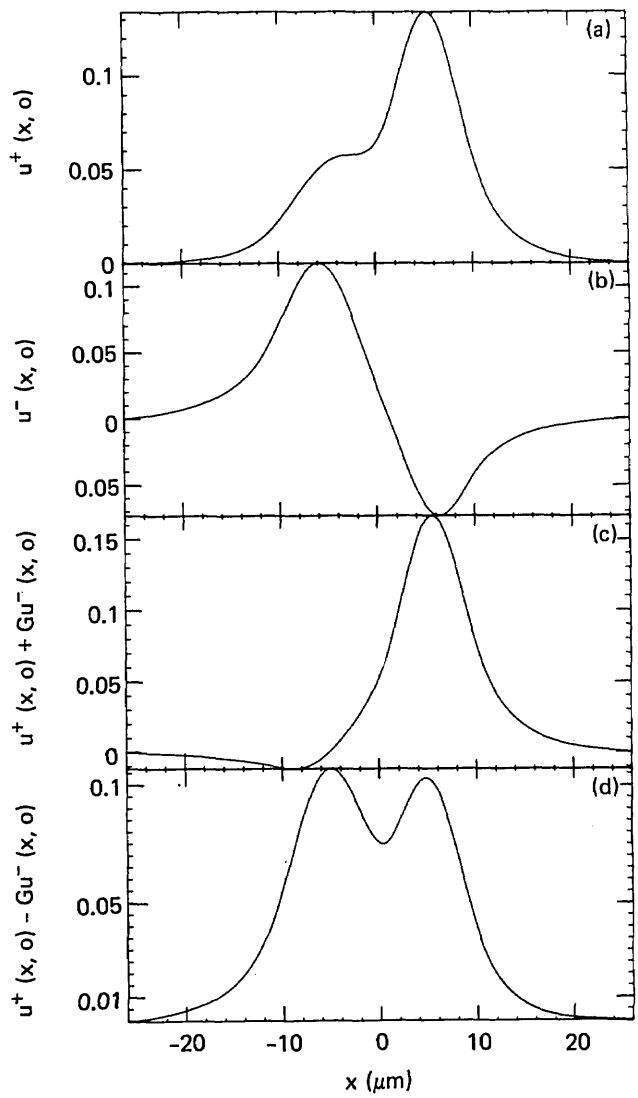

Fig. 8. Two nonidentical single-mode fibers with cores in contact. Linear combination of normal-mode eigenfunctions choosen to maximize power in one fiber. (a) $u^+(x, 0)$, (b) $u^-(x, 0)$, (c) $u^+(x, 0) + Gu^-(x, 0)$, (d) $u^+(x, 0) - Gu^-(x, 0)$, where $G = 0.4662$.

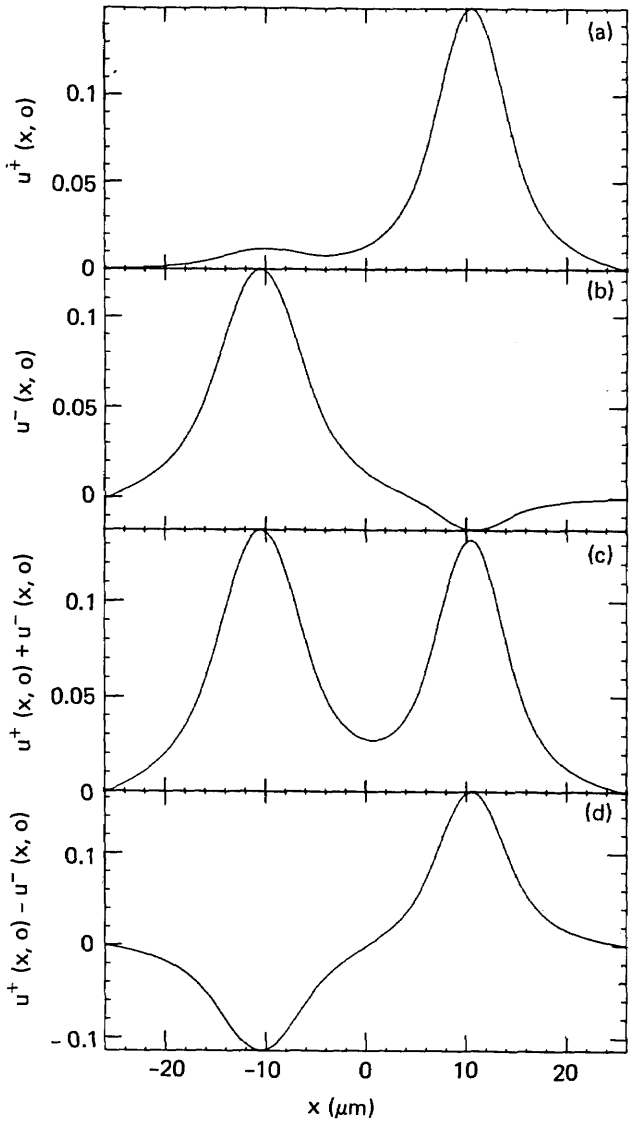

Fig. 9. Two nonidentical single-mode fibers at greater separation. (a) $u^+(x,0)$, (b) $u^-(x,0)$, (c) sum, (d) difference. Normal-mode eigenfunctions resemble eigenfunctions for isolated fibers. Sum and difference are no longer localized on one fiber.

one would conclude that, to address the problem of cross talk between two parallel multimode optical fibers, it is essential to have quantitative information on the excitation of the various modes. If, on the other hand, the fibers are to function as a coupler, it is obvious that only the highest-order modes can couple in a reasonable distance.

Figures 4 and 5 show eigenfunctions for low-order ($n = 3$) and the highest-order ($n = 17$) even- and odd-parity normal modes. A zero denotes the centers of the respective waveguides. Also displayed is the sum $u_n^+(x) + u_n^-(x)$, which represents the field when there is maximum localization of power on one waveguide.

8. COUPLED SINGLE-MODE OPTICAL FIBERS WITH TRUNCATED PARABOLIC PROFILES

Coupled Identical Fibers

We consider first the coupling of identical single-mode fibers with local index profiles given by Eq. (41), with $a = 5\ \mu m$, $\Delta = 1.2469 \times 10^{-3}$, and $n_0 = 1.5$. The even- and odd-parity normal modes were excited separately by using $\mathcal{E}_0'(x, y) = \exp[-(x^2 + y^2)/2\sigma^2]$ and $\sigma = 3.26\ \mu m$ in Eq. (39). The propagation constants β'^+ and β'^- and the splitting $\Delta\beta^\pm = \beta'^+ - \beta'^-$, computed for $\lambda = 1\ \mu m$, $\Delta z = 5\ \mu m$, and $z = 0.512$ cm, are given in Table 3 for three values of the separation d.

For the two cases of finite separation, the coupling between fibers is clearly strong. Figure 6 shows the even- and odd-parity normal-mode eigenfunctions and their sum and difference for $d = 10\ \mu m$, which brings the two fiber cores into contact. The displacement x is measured along a line joining the centers of the two fibers. The fractional powers associated with fibers A and B, obtained by numerical integration, are $P_A = 0.03748$ and $P_B = 0.96252$ for the field in Fig. 6(c). For Fig. 6(d), the fractional powers are reversed, and the indicated fractional power transfer is $\Delta P = 0.92504$.

Coupled Nonidentical Fibers

For this example fiber A parameters were retained, but fiber B parameters were changed to $a = 6\ \mu m$ and $\Delta = 0.8666 \times$

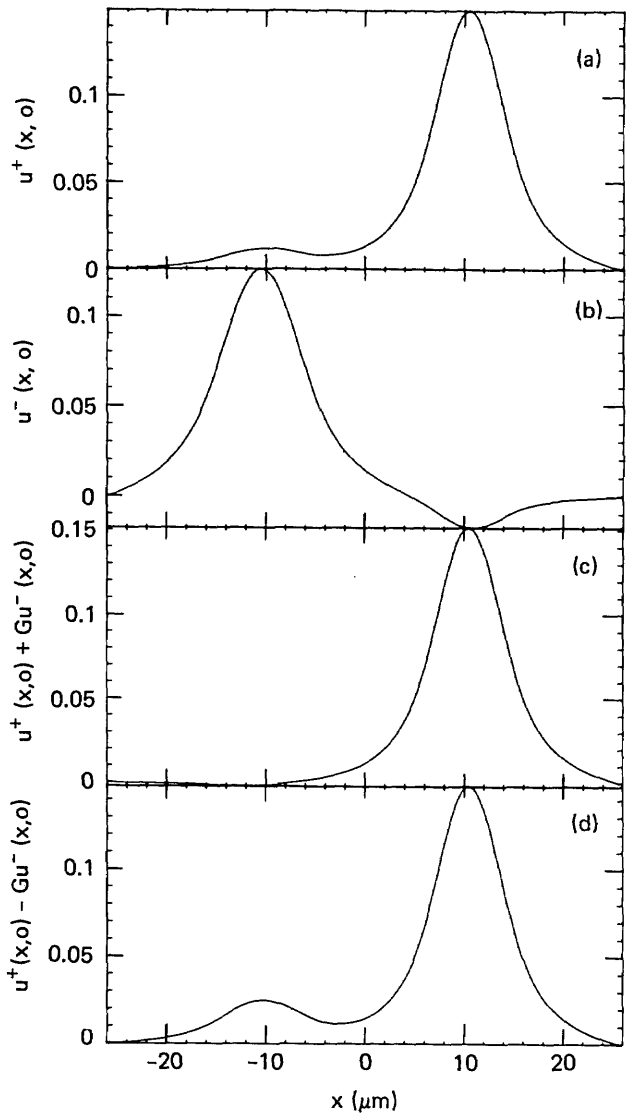

Fig. 10. Two nonidentical single-mode fibers at greater separation. Linear combination of normal-mode eigenfunctions chosen to maximize power on one fiber. (a) $u^+(x,0)$, (b) $u^-(x,0)$, (c) $u^+(x,0) + Gu^-(x,0)$, (d) $u^+(x,0) - Gu^-(x,0)$, where $G = 0.1055$.

10^{-3}. For the latter fiber in isolation, $\beta' = 19.095\ \text{cm}^{-1}$. The propagation constants for three separations are given in Table 4. It was not possible to excite separately the normal modes corresponding to $u^+(x, y)$ and $u^-(x, y)$ with an initial condition of the form of Eq. (39). However, the splitting $\Delta\beta^{\pm}$ was sufficiently large that both resonances could be resolved with ease.

Figure 7 shows plots of the normal-mode eigenfunctions $u^+(x, 0)$ and $u^-(x, 0)$ and their sum and difference for $d = 11$ μm, which brings the two cores into contact with each other. The normal-mode eigenfunctions display the quasi-even and -odd parity referred to in Section 4. The sum and difference of the eigenfunctions display an asymmetric concentration of power on the respective fibers. The power fractions associated with Figs. 7(c) and 7(d) are $P_A = 0.86815$, $P_B = 0.13185$ and $P_A = 0.13758$, $P_B = 0.86242$, respectively. This corresponds to a fraction $\Delta P = 0.7363$ of total power transferred.

In Section 5 it was shown that the fraction of power on one fiber could be maximized by choosing the field as the linear

Table 5. Propagation Constants for Coupled Identical Three-Mode Fibers with Truncated Parabolic-Index Profiles as a Function of Separation d

Separation d (μm)	Mode m n	Even Parity β'^{+}_{mn} (cm^{-1})	Odd Parity β'^{-}_{mn} (cm^{-1})
∞	0 0	131.6168	131.6168
	1 0	37.3493	37.3493
	0 1	37.3493	37.3493
20	0 0	131.6725	131.5626
	1 0	38.5693	35.9167
	0 1	37.5600	37.1124
16	0 0	132.0747	131.1756
	1 0	41.4777	32.4936
	0 1	38.2594	36.4229
14	0 0	132.9912	130.3899
	1 0	45.0429	28.2560
	0 1	39.2788	35.4268

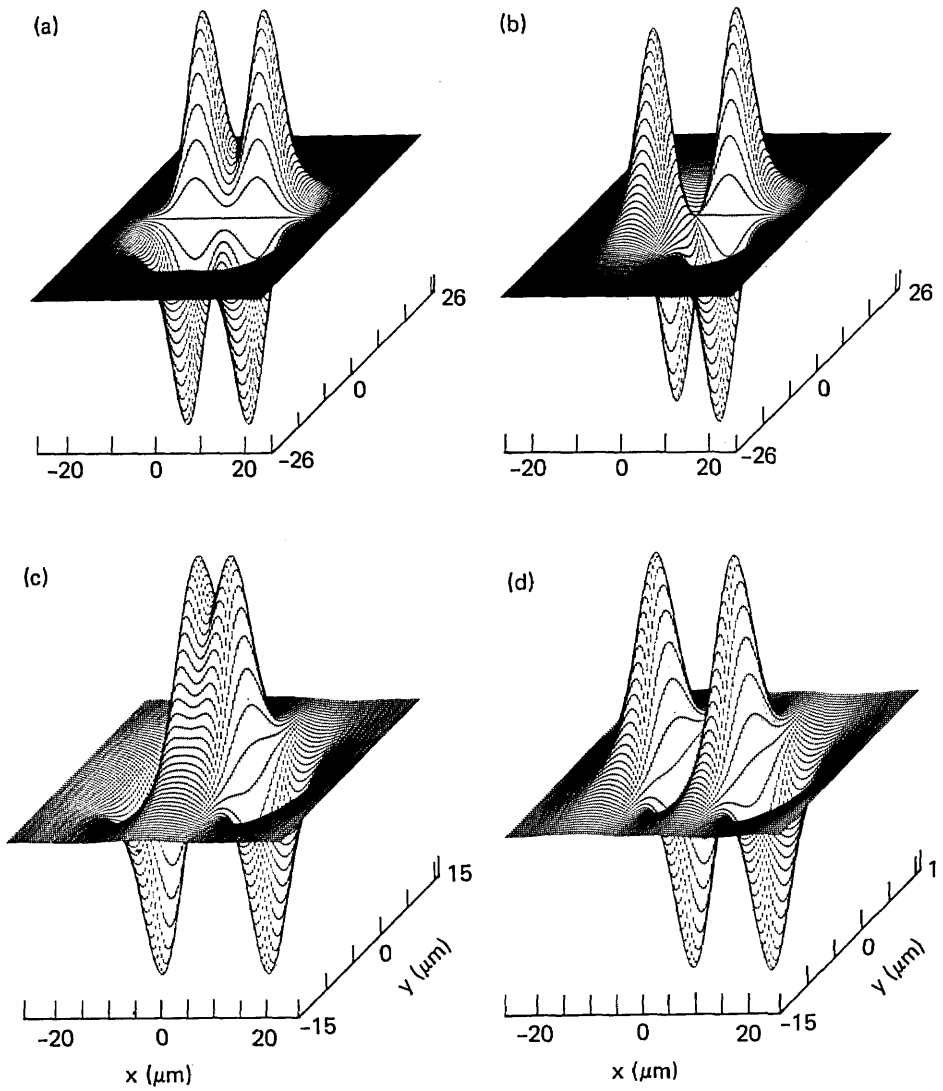

Fig. 11. Normal-mode eigenfunctions for coupled identical three-mode fibers with truncated parabolic profiles. Examples of both even- (+) and odd- (−) parity functions are shown. (a) $u^{+}_{01}(x, y)$, (b) $u^{-}_{01}(x, y)$, (c) $u^{+}_{10}(x, y)$, (d) $u^{-}_{10}(x, y)$. The eigenfunctions $u^{\pm}_{mn}(x, y)$ resemble symmetric and antisymmetric combinations of distorted versions of the functions $u^{0}_{mn}(x, y) = \exp[-(x^2 + y^2)/2\sigma_a]H_m(x/\sigma_a)H_n(y/\sigma_a)$, where $H_m(x/\sigma_a)$ is a Hermite polynomial.

combination $u^+(x, y) + Gu^-(x, y)$, with G determined by Eq. (33). This maximal concentration of power on one fiber, however, would take place at the expense of reduced power transfer. This is apparent from Figs. 8(c) and 8(d), which are plots of $u^+(x, 0) + Gu^-(x, 0)$ and $u^+(x, 0) - Gu^-(x, 0)$, for $G = 0.4662$, obtained from Eq. (33). The power fractions corresponding to Fig. 9(c) are $P_A = 0.04028$ and $P_B = 0.95972$, and those corresponding to Fig. 9(d) are $P_A = 0.60091$ and $P_B = 0.39909$. The associated fraction of power transferred is $\Delta P = 0.5606$. The field patterns in Figs. 8(c) and 8(d) and the associated fractional power transfer are certainly more representative of a functioning coupler than those associated with Figs. 7(c) and 7(d).

Figure 9 shows normal-mode eigenfunctions and their sum and difference for the same fiber combination at a separation of 21 μm. The eigenfunctions now closely resemble those for isolated fibers, and the corresponding propagation constants are only slightly perturbed from their values for infinite separation (see Table 4). The field configurations in Figs. 9(c) and 9(d) correspond to a maximum transfer of power. For Fig. 9(c), the power distribution is $P_A = 0.59929$ and $P_B = 0.40071$, and for Fig. 9(d), $P_A = 0.39910$ and $P_B = 0.60090$. The corresponding fractional power transfer is 0.200. Both field configurations, however, correspond to an almost equal sharing of power between the fibers and therefore do not accurately represent the field conditions in a functioning coupler.

On the other hand, Figs. 10(c) and 10(d), which show the normal-mode superpositions $u^+(x, y) \pm Gu^-(x, y)$, where $G = 0.1055$, as determined by Eq. (39), more nearly represent the field conditions in a functioning coupler. The power fractions corresponding to Figs. 11(a) and 11(b) are $P_A = 0.00361$, $P_B = 0.99639$ and $P_A = 0.0469$, $P_B = 0.9531$, respectively. The associated fractional power transfer is 0.043.

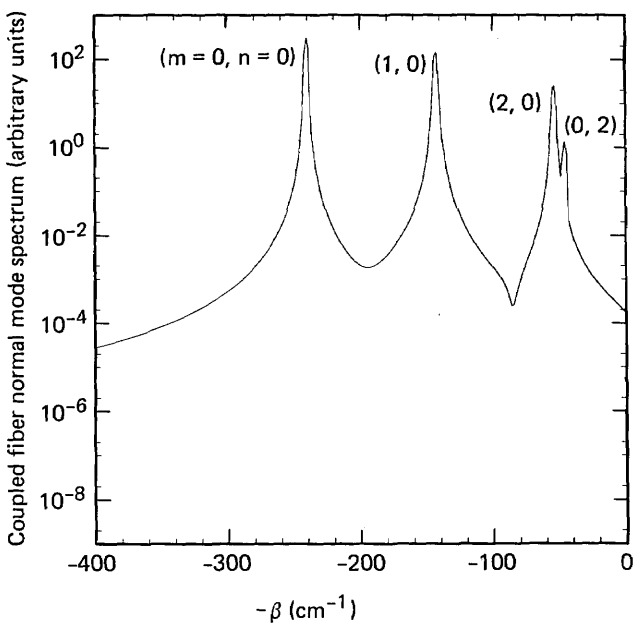

Fig. 12. One of the spectrum functions used to identify the normal modes of coupled identical six-mode fibers. Indices of modes excited are indicated.

Table 6. Propagation Constants for Coupled Identical Six-Mode Fibers with Truncated Parabolic-Index Profiles

Separation d (μm)	Mode m	Mode n	Even Parity β'^{+}_{mn} (cm^{-1})	Odd Parity β'^{-}_{mn} (cm^{-1})
∞	0	0	240.49913	240.49913
	1	0	141.09882	141.09882
	0	1	141.09882	141.09882
	1	1	47.22126	47.22126
	2	0	44.46053	44.46053
	0	2	44.46053	44.46053
17	0	0	240.67743	240.33552
	1	0	143.23196	139.20690
	0	1	143.31982	140.88743
	1	1	47.14235	41.83730
	2	0	54.15728	36.51435
	0	2	46.0326	45.54026

9. COUPLING OF IDENTICAL THREE-MODE FIBERS

For this case the fiber profiles are described by Eq. (41) with $a = 7$ μm and $\Delta = 2.43805 \times 10^{-3}$. For an isolated fiber such a profile permits three bound modes, two of which are degenerate.

The indices m, n, which designate the eigenfunction set of Eq. (42) for an isolated fiber, are also good quantum numbers when two fibers are brought together because the functions of Eq. (42) exhibit the symmetry with respect to reflection through the x and y axes that will be required of the normal modes. Hence the normal modes for the coupled fiber system can be designated by indices m and n and by parity $\pm$. The eigenfunctions can in turn be written as $u^{\pm}_{mn}(x, y)$. The propagation constants $\beta^{\pm}_{mn}$ as functions of fiber separation d appear in Table 5 for all bound normal modes. Figure 11 contains plots of the eigenfunctions $u^{+}_{01}(x, y)$, $u^{+}_{10}(x, y)$, $u^{-}_{01}(x, y)$, and $u^{-}_{10}(x, y)$, which resemble symmetric and antisymmetric combinations of distorted versions of functions from the set of Eq. (42).

In Table 5 it will be observed that the splitting $\beta'^{+}_{01} - \beta'^{-}_{01}$ is always less than the splitting $\beta'^{+}_{10} - \beta'^{-}_{10}$. This is easily understood from Fig. 11 and Eq. (21): the functions $u^{+}_{01}(x, y)$ and $u^{-}_{01}(x, y)$ clearly exhibit less overlap than the functions $u^{+}_{10}(x, y)$ and $u^{-}_{10}(x, y)$.

10. COUPLING OF IDENTICAL SIX-MODE FIBERS

Here the parabolic profile of Eq. (41) was characterized by $a = 8.5$ μm and $\Delta = 3.586587 \times 10^{-3}$, which permits six bound modes for an isolated fiber. The modes of the combined system can be labeled according to the scheme used for the coupled three-mode fibers. Normal modes were generated several at a time by choosing $\mathcal{E}'_0(x, y)$ of Eq. (39) in the form

$$\mathcal{E}'_{0(x)} = (1 + x)f(x)\exp(-x^2/2\sigma_a^2)H_n(y/\sigma_a), \qquad (45)$$

where $f(x)$ is a well-behaved function, e.g., another Gaussian function. With Eq. (45), one can generate the bound normal modes corresponding to a single value of n and all values of m. The spectrum function $|\mathcal{P}(\beta)|$, for even-parity normal

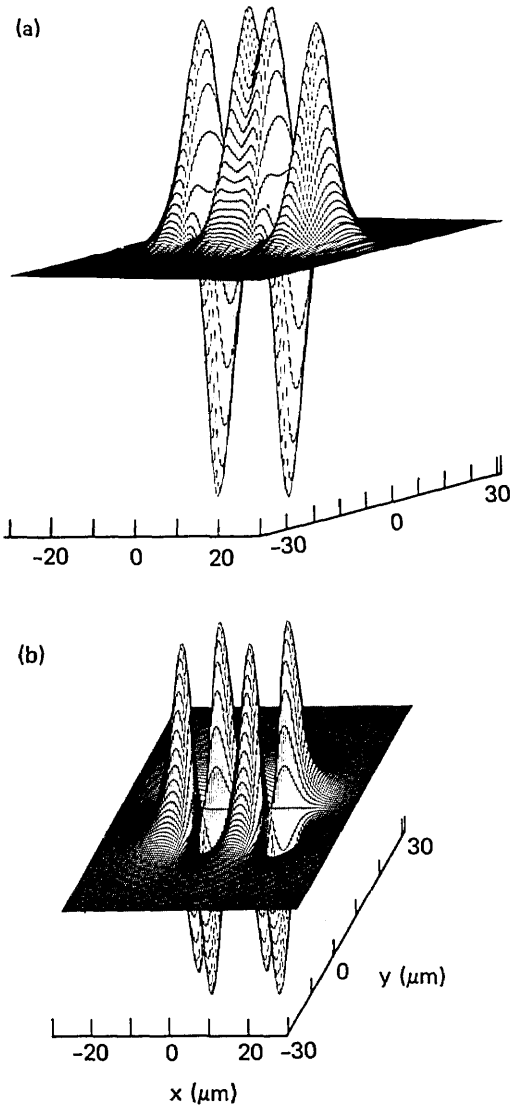

Fig. 13. Normal-mode eigenfunctions for coupled identical six-mode fibers with truncated parabolic profiles. (a) $u^{+}_{20}(x, y)$, (b) $u^{-}_{11}(x, y)$.

modes and $n = 0$ in Eq. (45), is shown in Fig. (12). The unexpected weak-satellite resonance corresponds to $u^{+}_{02}(x, y)$. It is excited because $u^{+}_{02}(x, y)$ has the same symmetry as $u^{+}_{20}(x, y)$. This accidental excitation of normal modes that do not correspond to the exciting set can be expected to occur more frequently as the number of bound modes of the coupled fibers increases, and it tends to complicate the analysis and identification of normal modes.

The propagation constants for the separations $d = \infty$ and $d = 17$ μm are given in Table 6 for all bound normal modes, and the normal-mode eigenfunctions $u^{+}_{20}(x, y)$ and $u^{-}_{11}(x, y)$ are shown in Fig. 13. From Table 6 it may be noted that for $d = \infty$ the mode with indices $(m, n) = (1, 1)$ does not belong to the degenerate set that includes modes (2, 0) and (0, 2), although all three modes would be degenerate for an infinite focusing medium or a highly multimode parabolic profile. The partial removal of degeneracy is due to the truncation of the parabolic profile. The degeneracy of the modes (2, 0) and (0, 2) is unaffected because of their symmetry. It will also be noted from Table 6 that the splitting $\Delta\beta^{\pm}$ is greater for those mode pairs whose basic orientation is in the x direction rather than in the y direction.

CONCLUSION

We have used the propagating beam method to determine the normal-mode properties of a variety of coupled waveguides of practical interest. The method is straightforward to apply, and it allows a complete characterization of such systems within the framework of the weak-guidance approximation. These results demonstrate the wide applicability of the propagating beam method to coupling problems in general and to the analysis of general waveguiding structures with two transverse dimensions.

ACKNOWLEDGMENT

This research was performed by the Lawrence Livermore National Laboratory, Livermore, California, under the auspices of the U.S. Department of Energy, contract no. W-7405-ENG-48.

REFERENCES

1. S. E. Miller, "Coupled wave theory and waveguide applications," Bell Syst. Tech. J. **33**, 661–719 (1954).
2. J. S. Cook, "Tapered velocity couplers," Bell Syst. Tech. J. **34**, 807–822 (1955).
3. A. G. Fox, "Wave coupling by warped normal modes," Bell Syst. Tech. J. **34**, 823–852 (1955).
4. W. H. Louisell, "Analysis of the single tapered mode coupler," Bell Syst. Tech. J. **34**, 853–870 (1955).
5. A. L. Jones, "Coupling of optical fibers and scattering in fibers," J. Opt. Soc. Am. **55**, 261–271 (1965).
6. R. Van Clooster and P. Phariseau, "The coupling of two parallel dielectric fibers. I. Basic equations," Physica **47**, 485–500 (1970).
7. R. Van Clooster and P. Phariseau, "The coupling of two parallel dielectric fibers. II. Characteristics of the coupling in two fibers," Physica **47**, 501–514 (1970).
8. D. Marcuse, "The coupling of degenerate modes in two parallel dielectric waveguides," Bell Syst. Tech. J. **50**, 1791–1816 (1971).
9. A. W. Snyder, "Coupled mode theory of optical fibers," J. Opt. Soc. Am. **62**, 1267–1277 (1972).
10. J. Arnaud, "Transverse coupling in fiber optics, Part IV: crosstalk" Bell Syst. Tech. J. **54**, 1431–1450 (1975).
11. A. H. Cherin and E. J. Murphy, "Quasi ray analysis of crosstalk," Bell Syst. Tech. J. **54**, 17–45 (1974).
12. W. Wijngaard, "Guided normal modes of two parallel circular dielectric rods." J. Opt. Soc. Am. **63**, 944–950 (1973).
13. C. Yeh, W. P. Brown, and R. Szejn, "Multimode inhomogenous fiber couplers," Appl. Opt. **18**, 489–495 (1979).
14. M. D. Feit and J. A. Fleck, Jr., "Light propagation in graded-index optical fibers," Appl. Opt. **17**, 3990–3998 (1978).
15. M. D. Feit and J. A. Fleck, Jr., "Computation of mode properties in optical fiber waveguides by propagating beam method," Appl. Opt. **19**, 1154–1164 (1980).
16. M. D. Feit and J. A. Fleck, Jr., "Mode properties and dispersion for two optical fiber index profiles by the propagating beam method," Appl. Opt. **19**, 3140–3150 (1980).
17. M. D. Feit and J. A. Fleck, Jr., "Mode properties of optical fibers with lossy components by the propagating beam method," Appl. Opt. **20**, *848–856 (1981).*
18. J. A. Arnaud, *Beam and Fiber Optics* (Academic, New York, 1976), pp. 211–216.